The Ka-Band Receiver for the QUIJOTE Experiment

Juan L. Cano, Enrique Villa, Beatriz Aja,
Luisa de la Fuente, Eduardo Artal
Dep. Ingeniería de Comunicaciones
Universidad de Cantabria
39005 Santander, Spain
juanluis.cano@unican.es

Robert Watson, Edward Blackhurst, John Edgley,
Colin Baines
Jodrell Bank Centre for Astrophysics
University of Manchester
Manchester, M13 9PL, United Kingdom

***Abstract* — The 26-36 GHz receiver for a radio astronomy radiometer, to characterize the polarization of the Cosmic Microwave Background, is presented. This receiver is based on very low noise cryogenically cooled amplifiers in the front-end module, while in the back-end module a broadband amplification and direct detection chain is operated at room temperature. Noise temperature of the low-noise amplifier (LNA) is 19 K when cooled at 18 K. Experimental results show a good sensitivity of the complete receiver with an effective bandwidth around 8 GHz. Moreover, output detected voltages agree with estimated values.**

Keywords: radiometer; radiometry; radio astronomy; very low noise receivers; cryogenic amplifiers; HEMT; InP

I. INTRODUCTION

The QUIJOTE experiment, currently under installation at El Teide observatory (Tenerife, Spain), is a radio astronomy project aimed to characterize the polarization of the Cosmic Microwave Background and other galactic and extragalactic emission processes. These measurements will complement those obtained by Planck mission, correcting galactic contamination.

The instrument consists of five receivers (pixels) covering different frequency bands: two in the 10 – 14 GHz range, two in the 14 – 20 GHz range, and one pixel in the 26 – 36 GHz range. In the last frequency band, the signal coming from the sky goes through the feedhorn to a rotating waveguide polar modulator [1]. This component modulates the polarization of the incoming signal and, at the same time, reduces the low frequency gain fluctuations at the output signal. After the modulator, the signal is separated into its orthogonal components in the orthomode transducer [2], which come out into the front-end module (FEM). The FEM provides high gain and very low noise to the system through indium-phosphide based cryogenic low-noise amplifiers (one per signal component). The back-end module (BEM), located just after the FEM, provides further RF amplification, band filtering, detection and dc amplification to supply adequate signal levels to the data acquisition electronics (DAE). A simplified sketch of the highest frequency pixel is shown in Fig. 1.

This paper presents experimental results obtained during the integration tests of the two modules, the front-end module cooled at cryogenic temperature (T = 18 K) connected to the back-end module at room temperature (T = 296 K), and detailed information about the subsystems design.

This work has been funded by the Ministerio de Ciencia e Innovación (Spain) under Astronomy and Astrophysics research programme, reference AYA2007-68058-C03.

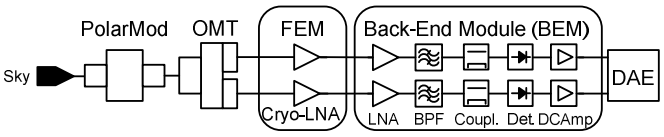

Figure 1. Radiometer configuration for the Ka-band pixel. The polar modulator and the orthomode transducer are also cryogenically cooled.

II. MODULES DESIGN

A. The Front-End Module (FEM)

The front-end module is designed to provide high gain and very low noise at cryogenic temperatures with minimum power consumption. In order to fulfill all these requirements this module uses state-of-the-art low noise indium-phosphide (InP) HEMT technology. Specifically, this module includes a MMIC low-noise amplifier, designed originally for the FARADAY project, using 0.1 μm InP HEMT technology from NGST [3], [4].

The module, machined in brass, is completed with suitable designed waveguide (WR-28)-to-microstrip transitions at both ports. The whole subsystem performs an average gain around 37 dB and average noise temperature around 19 K when cooled at 15 K, with only 56 mW of power consumption. Fig. 2 shows a picture of the front-end module LNA

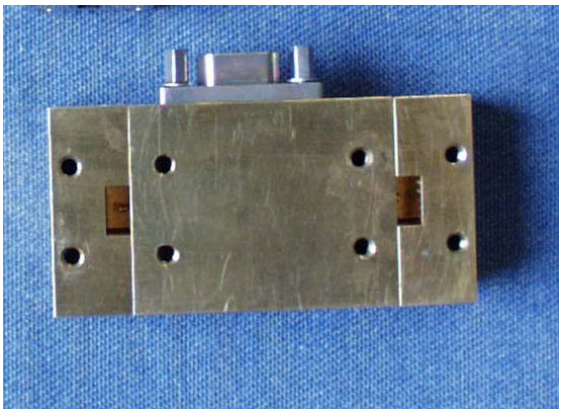

Figure 2. Front-end module LNA (26-36 GHz)

B. *The Back-End Module (BEM)*

The back-end module is equipped with a WR-28 flange at the input to enable direct waveguide connection with the FEM and thus minimizing transmission losses. First components are two amplification stages. Since the noise requirements are not very restrictive for this subsystem, commercial low-noise amplifiers are selected for this module. The MMIC chip models AMMC-6241 from Avago Technologies and ALH-140 from Velocium are cascaded to achieve around 32 dB of RF gain.

A band pass filter in microstrip technology on Alumina substrate (height h = 0.254 mm; ε_r= 9.9) defines the operational bandwidth. A microstrip forward directional coupler provides a RF signal sample at the output while the remaining RF signal is directed to the detector. The coupling factor is 13 dB. Finally, the detector converts the incoming RF power into dc voltage that is conveniently amplified in a subsequent stage designed with regular operational amplifiers. The detection is made using a zero-bias Schottky diode. Fig. 3 shows a sketch of the radiofrequency elements in the back-end module. The dc amplifier is not showed.

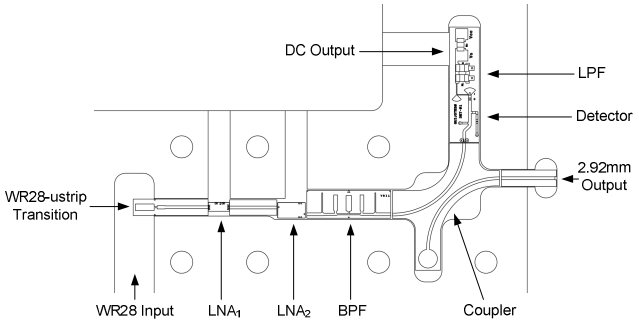

Figure 3. Sketch of the RF components within the BEM

A picture of the radiofrequency components inside the back-end module is in Fig. 4.

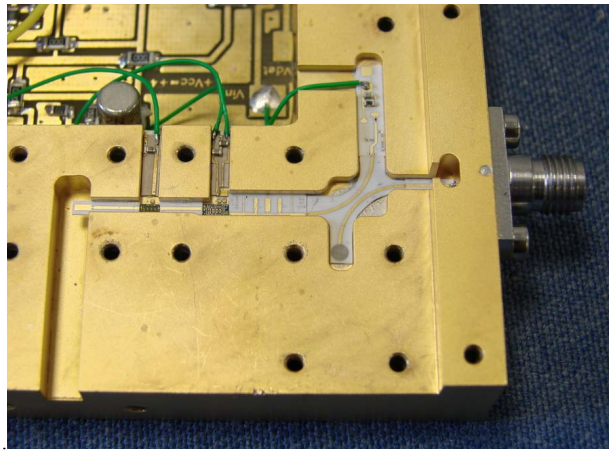

Figure 4. Picture of RF components inside the 26-36 GHz BEM

The RF sample output (2.92 mm connector in Fig. 4) is used for monitoring purposes, i.e. to test the full RF receiver response before direct detection by the Schottky diode.

III. MEASUREMENT SETUP

In order to measure the performance of the front-end module connected to the back-end module under operating conditions, the FEM was installed inside the cryostat Dewar. Due to the lack of waveguide ports for the cryostat, the FEM was equipped with waveguide-to-coaxial (2.4 mm) transitions. A picture of the assembly within the cryostat is in Fig. 5. The back-end module, outside the cryostat, was connected to the front-end module using a coaxial line and a 20-dB coaxial attenuator. This attenuator, also placed outside the cryostat, avoids the detector saturation due to high power signal at the system input during the test campaign (a matched load at the input at room temperature produces enough noise power to saturate the detector). However, under normal operation conditions when the receiver is installed in the radiotelescope signal level is lower and the 20-dB attenuator is removed.

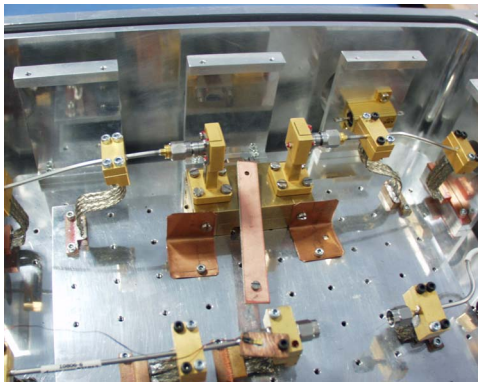

Figure 5. Picture of the FEM installed inside the cryostat Dewar.

For the RF transmission test (S_{21} parameter) and effective bandwidth calculation, an E8364A network analyzer (Agilent Technologies) is connected between the cryostat input port and the BEM coupled port. The network analyzer is set up with an output power of -40 dBm. From the measured gain, the receiver effective bandwidth is defined by (1) [5].

$$BW_{eff} = \frac{\left|\int G(f)df\right|^2}{\int |G(f)|^2 df} \tag{1}$$

Where $G(f)$ is the receiver power gain, $G(f) = |S_{21}|^2$, at each frequency point. The RF-to-dc performance is characterized measuring the detected dc voltage at BEM output versus the input frequency at a fixed input power. The receiver sensitivity is tested versus input power at a fixed input frequency. For these tests a sweep generator model 83650B from Hewlett-Packard is connected to the cryostat coaxial port, while the detected voltage is measured using a voltmeter, being both instruments controlled by a computer. A receiver overall sensitivity has been defined and calculated by using (2).

$$S(dB) = 10\log(V_{out} - V_{offset}) - P_{in} \tag{2}$$

Where V_{out} is the output detected voltage, V_{offset} is the output detected voltage when the generator is switched-off (both voltages are in mV), and P_{in} is the input power in dBm.

IV. Measurement Results

In Fig. 6, the RF transmission characteristic (gain $|S_{21}|^2$) of the whole system is shown. From this curve the effective bandwidth is calculated obtaining a result of BW_{eff} = 8.02 GHz.

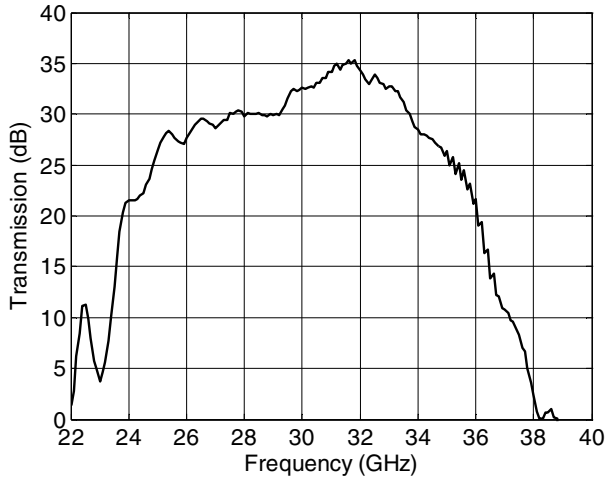

Figure 6. Receiver transmission curve (20 dB attenuator inserted).

The detected voltage versus input frequency is measured for different powers delivered by the generator. The results of these measurements are plotted in Fig. 7. From this plot, it can be seen that the system starts to saturate at around -57 dBm input power even with the 20 dB coaxial attenuator placed between the front-end module and the back-end module.

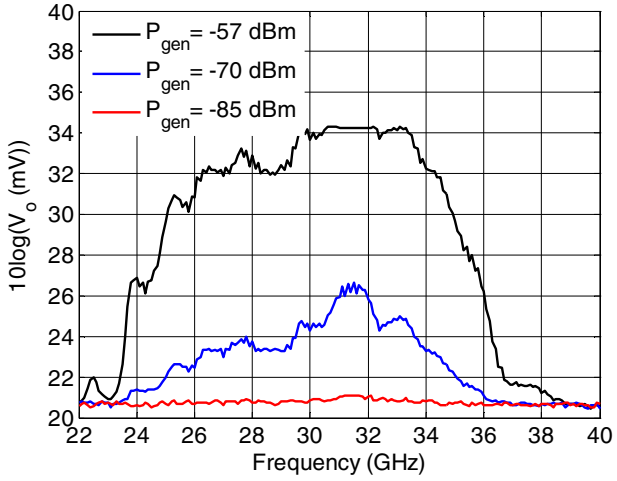

Figure 7. Detected voltage for different generator power values: P_{gan} = -57 dBm (black line), P_{gan} = -70 dBm (blue line), P_{gan} = -85 dBm (red line).

Finally, the system sensitivity defined in (2) is shown in the plot of Fig. 8 versus input power, at the center frequency and at the frequency band edges. The input power has been corrected with the input cable losses.

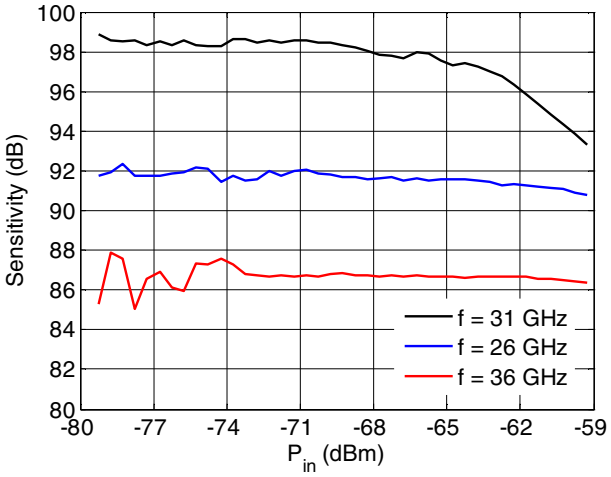

Figure 8. System sensitivity versus input power for different frequencies: f = 26 GHz (blue line), f = 31 GHz (black line), f = 36 GHz (red line).

V. Power Budget Estimation

In order to check the radiometer performance, the noise power level at the system output was measured and compared with calculated values. Calculations were made using the available test data of individual subsystems obtained during a previous test campaign.

With a matched load placed at the cryostat input, therefore at a temperature around T = 300 K, a front-end module noise temperature of T_e = 19 K, and an effective bandwidth of B = 8.02 GHz, then the equivalent noise power at the FEM input is given by (3). The test setup is depicted in Fig. 9.

$$P_{in} = k(T + T_e)B \tag{3}$$

Where k is the Boltzmann's constant. Equation (3) gives an input power of P_{in} = -73.5 dBm. Taking into account front-end module and back-end module gains (output at RF coupled port), transmission losses of the coaxial cables and the 20-dB attenuator, at the center frequency of 31 GHz (32.7 dB from Fig. 6), the calculated power at the system output is -40.8 dBm. This value agrees well with the measured value of -41.7 dBm, which has been measured using a power meter model E4418B from Agilent Technologies.

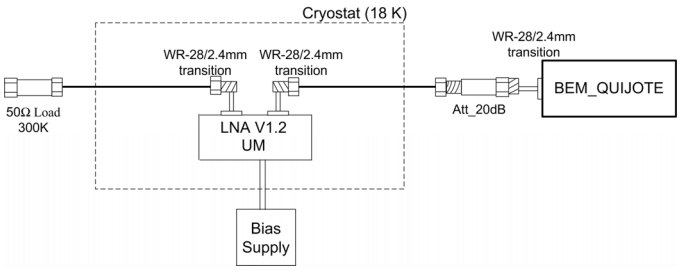

Figure 9. Test setup for noise power tests.

If the detection stage is included in this calculation, the signal is routed through the direct arm of the coupler and then

the noise power at the detector input would be -27.8 dBm. The diode detector has a sensitivity around S = 1000 mV/mW, which produces a detected voltage of V_{det} = 1.66 mV. The dc amplifier was adjusted to have a voltage gain of G_V = 116, which raises the output voltage to V_o = 192.5 mV. This last value, 10 log[V_o(mV)] = 22.8, agrees with the experimental results showed in Fig. 7 for a generator power slightly lower than -70 dBm, as it is the case (calculated input noise power value of -73.5 dBm).

VI. CONCLUSIONS

The Ka-band radio astronomy receiver is a broadband and very low noise system for operation from 26 to 36 GHz. The experimental results obtained during the test campaign carried out with the whole RF chain assembled, i.e. the front-end module cooled at cryogenic temperature connected to the back-end module at room temperature, have demonstrated a high sensitivity of the receiver, achieving a large effective bandwidth of about 8 GHz. Output detected values obtained by experimental tests have been checked through calculations, using the collected data from the individual subsystems of the receiver. According to these results, the receiver system performs as expected under test conditions and it is foreseen to work properly during normal operation in the observatory.

ACKNOWLEDGMENT

The authors thank Eva Cuerno and Ana Pérez for their assistance in the assembly of the circuits.

REFERENCES

[1] E. Artal, L. de la Fuente, B. Aja, J.L. Cano, E. Villa, R. Hoyland, J.A. Rubiño-Martin, and R. Genova, "Cosmic Microwave Background Polarization Receivers: QUIJOTE Experiment", Proc. 40th European Microwave Conference, Paris, 2010, pp. 497-500.

[2] J.L. Cano, A. Tribak, R. Hoyland, A. Mediavilla, and E. Artal, "Full band waveguide turnstile junction orthomode transducer with phase matched outputs", Int. J. RF and Microwave CAE, vol. 20, no. 3, May 2010, pp. 333-341.

[3] A. Cremonini, S. Mariotti, V. Natale, R. Nesti, A. Orfei, G. Tofani, D. Kettle, R. Witvers, and J. G. B. de Vaate, "State of the art MMIC InP LNA realizations and applications in FARADAY array receivers", IEEE Mediterranean Electrotechnical Conf., MELECON 2006, Malaga, Spain, July 2006, pp. 561-564.

[4] D. Kettle, N. Roddis, and R. Sloan, "A lattice matched InP chip set for a Ka band radiometer", IEEE MTT-S, June 2005, pp. 1133-1136.

[5] M. E. Tiuri,"Radio Astronomy Receivers",IEEE Transactions on Antenas and Propagation, pp 930-938, Dec. 1964.